

Chiya Ahmed Basha¹
Muniasamy Sathish
Shankar²
Vijayasekaran
Boovaragavan^{1,3}
Somasundara Rao
Pullabhotla²

¹ Central Electrochemical
Research Institute, Tamilnadu,
India.

² Vellore Institute of Technology,
Tamilnadu, India.

³ Chemical Engineering,
Tennessee Technological
University, Tennessee, USA.

Research Article

Computation of Current Distributions using FEMLAB

An efficient method for the computation of current density and surface concentration distributions in electrochemical processes is analyzed using the commercial mathematical software FEMLAB. To illustrate the utility of the software, the procedure is applied to some realistic problems encountered in electrochemical engineering, such as current distribution in a continuous moving electrode, parallel plate electrode, hull cell, curvilinear hull cell, thin layer galvanic cell, through-hole plating, and a recessed disc electrode. The model equations of the above cases are considered and their implementations into the software, FEMLAB, are analyzed. The technique is attractive because it involves a systematic way of coupling equations to perform case studies.

Keywords: Electrochemical processes, Mathematical analysis, Modeling

Received: September 09, 2008; *revised:* October 23, 2008; *accepted:* October 26, 2008

DOI: 10.1002/ceat.200800458

1 Introduction

The knowledge of current distribution in various geometrical configurations of electrolytic cells is important both for the analysis of data obtained in electrochemical experiments, and for design and scale-up. Owing to the large number of variables, the nature of the problem is complex. In order to design a reactor and also to understand the performance in this more complicated process, it is essential to simultaneously take into account several phenomena that influence the current distribution. Thus, it is necessary to solve for the concentration fields and the potential field simultaneously. The solution of such problems is often termed the tertiary current distribution. Since the mathematical methods leading to an analytical solution are usually not applicable in more complicated cases, the only possibility remaining is to use a semi-analytical software approach.

Tertiary current distributions have not been treated extensively. Newman [1] has discussed this class of problem, indicating how to treat current distribution in cells where the potential distribution in the bulk of the solution and the concentration distribution in the diffusion layer must be calculated simultaneously. These ideas [2] were applied to other electrochemical cell geometries such as current distribution on plane parallel electrodes, rotating spherical electrodes, continuous moving sheet electrodes, etc. The computation methods

used in most of these cases are one or the other form of Newman's technique. In recent work, semi-analytical methods or numerical methods have been used for calculating current density distributions with respect to diffusion, migration, and laminar convection, including high velocities and electrochemical reaction kinetics [3–17].

In this work, the authors used the mathematical software, FEMLAB, instead of the semi-analytical approach to represent the current distribution. The technique is much simpler to solve surface concentration and potential simultaneously. It is easier for most researchers to use commercially available software since they can treat a much larger range of conditions. The model equations encountered in some realistic problems in electrochemical engineering, such as current distribution in a continuous moving electrode, parallel plate electrode, hull cell, curvilinear hull cell, thin layer galvanic cell, through-hole plating, and recessed disc electrode, are considered and their implementations into the commercial mathematical software, FEMLAB, are analyzed. The semi-analytical approach is also indicated in section 4 for the current distribution computation for validation of FEMLAB results.

2 Mathematical Analysis

A simple model considered for the evaluation of current distributions involves the following assumptions: (i) a single cathodic reaction takes place at the cathode, (ii) the concentration overpotential and the activation overpotential at the counter electrode are zero, (iii) the transport and kinetic parameters do not vary in space or time, (iv) the presence of the cell wall and the counter electrode do not affect the flow

Correspondence: Dr. C. A. Basha (cab_50@rediffmail.com, basha@cecri.res.in), Central Electrochemical Research Institute, Karaikudi-630006, Tamilnadu, India.

boundary layer on the working electrode, and (v) the physical properties of the electrolyte are constant and the cathode is of primary interest.

Assuming that we impose a specific voltage drop, E^1 , across the electrodes, the overall voltage balance can be written as:

$$E = \Phi_{\text{ohm}} + \eta_a + \eta_c \quad (1)$$

where E is the difference between the applied cell voltage and the thermodynamic equilibrium cell voltage. Φ_{ohm} is the ohmic voltage drop, η_a and η_c are the voltage drops due to activation polarization (i.e., kinetic effects) and concentration polarization (due to concentration gradients between the electrode surface and the bulk electrolyte), respectively.

The polarization equation is necessary to express the dependence of the local rate of the reaction on the various concentrations and on the potential jump at the interface. The situation is the same here as in chemical kinetics or heterogeneous catalysis. It is common to use the Butler-Volmer equation for electrode kinetics of the form for metal/ion systems:

$$i = i_0 \left(\frac{C_S}{C_\infty} \right)^\gamma \left[\exp\left(\frac{anF}{RT} \eta_a \right) - \exp\left(-\frac{\beta nF}{RT} \eta_a \right) \right] \quad (2)$$

where i_0 is the exchange current density, and a , β , and γ are kinetic parameters.

In view of the assumption of an excess of supporting electrolyte, the potential difference associated with the concentration variation is commonly written in terms of concentration overpotential as follows:

$$\eta_c = \frac{RT}{nF} \ln C_S \quad (3)$$

The diffusion process is governed by a partial differential equation that describes the way in which the concentration of the electrochemically active species changes with respect to the distance along the working electrode. It is fortuitous that similar diffusion phenomena, and hence equations, arise in many areas of science and engineering, and in particular, describe the uptake of a species in adsorbent or catalyst particles. Thus, the steady-state laminar convective diffusion equation, $\mathbf{V} \cdot (\nabla C) = D \nabla^2 C$, is used to describe the transport of the reactive ion from the bulk to the electrode surface. The choice of spatial coordinate and the boundary conditions depend on the electrode geometry. The boundary conditions will be discussed separately for each of the cell geometries.

In the electrolytic cell, the ohmic potential drop across the concentration boundary layer is negligibly small compared to the ohmic potential drop across the bulk of the electrolyte. Therefore, the potential drop across the electrolyte is governed by the Laplace equation, $\nabla^2 \Phi$, where $\Phi(x, y)$ represents the local electrical potential.

Thus, to determine the current density and concentration distributions along the electrode, the convective diffusion

equation and the Laplace equation must be solved simultaneously along with the electrochemical kinetics, using suitable geometry-dependent boundary conditions.

3 Model Equations

3.1 Continuous Moving Sheet Electrode

Electrochemical processes such as electrolysis of brine and electroplating of sheet metals and wires [18] make use of continuous moving electrodes. Consider one side of a continuous semi-infinite flat sheet electrode moving with a constant velocity, U_s , through an otherwise undisturbed electrolyte as shown in Fig. 1. The sheet enters the cell through a watertight slot at one end of the cell and leaves the cell at the opposite side through a second slot. The motion of the solid surface induces a flow of electrolyte in the direction of the sheet. The electrode velocity is high so that the boundary layer approximation can be used to describe the electrolyte flow near the electrode surface. The steady-state laminar convective diffusion equation for a continuous moving sheet is:

$$U \frac{\partial C}{\partial x} + V \frac{\partial C}{\partial y} = D \frac{\partial^2 C}{\partial y^2} \quad (4)$$

where U and V are the velocity components, and the choice of spatial coordinate and the boundary conditions depend on the electrode geometry. Assume the velocity variation in V is negligible and the velocity profile assumed in this case was $V = 0$ and $U = U_s$. The boundary conditions at the walls, the anode ($y = b$) and the cathode ($y = 0$) are:

$$C(b, y) = C(L, b) = C_\infty \quad (4-a)$$

$$D \frac{\partial C(x, y)}{\partial y} \Big|_{y=0} = \frac{i(x)}{nF} \quad (4-b)$$

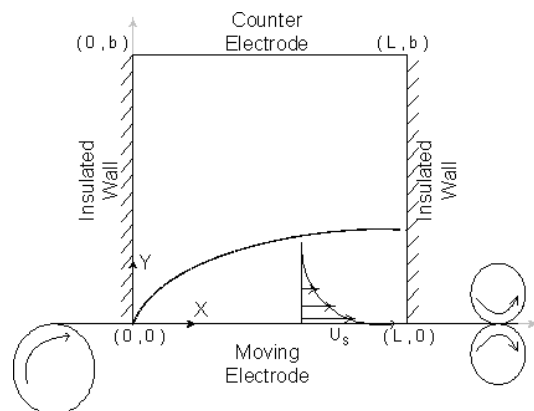


Figure 1. Schematic diagram of a continuous moving sheet electrode process.

1) List of symbols at the end of the paper.

The following boundary conditions were used to solve the potential field expressed by the Laplace equation:

$$\frac{\partial \phi}{\partial x} = 0 \text{ at } x = 0 \quad (5-a)$$

$$\text{and } \frac{\partial \phi}{\partial x} = 0, \text{ } x = L \text{ for } 0 \leq y \leq b \quad (5-b)$$

$$\Phi = 0 \text{ at } y = b \text{ for } 0 \leq x \leq L \quad (5-c)$$

$$\frac{\partial \phi}{\partial y} = \frac{-i}{\kappa} \text{ at } y = 0 \text{ for } 0 \leq x \leq L \quad (5-d)$$

3.2 Electroplating of a Through-Hole

We now consider the electroplating of high aspect ratio through-holes as shown in Fig. 2. Plating inside through-holes and crevices is critically important for innumerable technological applications [19]. High-density circuits require thicker boards with longer, smaller diameter holes. These trends make it difficult to achieve uniform plating due to severe mass transfer limitations [20]. The steady-state diffusion equation for laminar convective diffusion in circular cylindrical coordinates can be written as:

$$V_z(r) \frac{\partial C}{\partial z} = D \left[\frac{\partial^2 C}{\partial r^2} + \frac{1}{r} \frac{\partial C}{\partial r} \right] \quad (6)$$

where r and z are radial and axial distances. For small values of z such that $zD/2\langle V_z \rangle R_0^2 < 0.01$, Leveque [21] recognized that there is a diffusion layer near the tube wall where the second term in the brackets of Eq. (6) becomes much smaller than the first and the electrolyte velocity is approximately linear with distance from the tube wall.

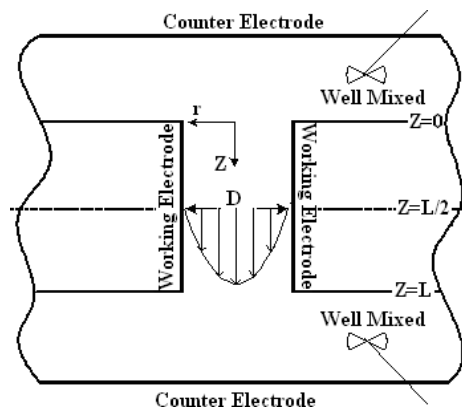


Figure 2. Definition sketch of a through-hole system under consideration.

By inserting these approximations into Eq. (6), one obtains:

$$V_z(y) \frac{\partial C}{\partial z} = D \frac{\partial^2 C}{\partial y^2} \quad (7)$$

$$\text{where } V_z(y) = \frac{4 \langle V_z \rangle}{R_0} y \quad (7-a)$$

and y is the normalized radial distance from the through-hole wall, $y = (R_0 - r)$. $\langle V_z \rangle$ is the average electrolyte velocity in the axial direction. In these situations, the boundary conditions are:

$$C = C_\infty \text{ at } y = R_0 \text{ for } z > 0 \quad (7-b)$$

$$C = C_\infty \text{ at } 0 \leq y \leq R_0 \text{ for } z \leq 0, z > L \quad (7-c)$$

$$\frac{\partial C}{\partial y} = \frac{i(z)}{nFD} \text{ at } y = 0 \text{ for } 0 \leq z \leq L \quad (7-d)$$

For the Laplace equation, the following boundary conditions are applied:

$$\frac{\partial \phi}{\partial y} = 0 \text{ at } z = 0 \quad (8-a)$$

$$\text{and } \frac{\partial \phi}{\partial y} = 0 \text{ } z = L \text{ for } 0 \leq y \leq R_0 \quad (8-b)$$

$$\frac{\partial \phi}{\partial y} = \frac{-i(z)}{\kappa} \text{ at } 0 < z < L \text{ and } y = R_0 \quad (8-c)$$

3.3 Plane Parallel Electrodes

Many industrial electrochemical processes use channel flow between two plane parallel electrodes as shown in Fig. 3. Due to the importance of parallel electrodes, a great deal of effort has been devoted to describing the current distribution [22–24]. The boundary conditions at the insulating walls and at the

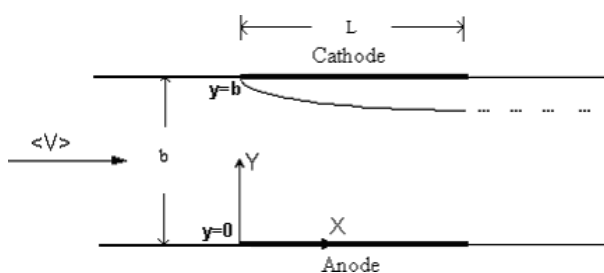


Figure 3. Locations of the plane parallel electrodes on the walls of the flow channel.

anode ($y = b$) are the same as in earlier cases, while the boundary conditions at the cathode ($y = 0$) are:

$$\frac{\partial C}{\partial y} = \frac{i}{nFD} \quad \text{at } y = 0 \quad \text{for } 0 < x < L \quad (9)$$

For this geometry, the Laplace equation is subjected to the following conditions:

$$\frac{\partial \phi}{\partial y} = 0 \quad \text{at } y = 0 \quad \text{for } x < 0 \quad \text{and } x > L \quad (10\text{-a})$$

$$\frac{\partial \phi}{\partial y} = \frac{-i}{\kappa} \quad \text{at } y = 0 \quad \text{for } 0 < x < L \quad (10\text{-b})$$

3.4 Hull Cell

The Hull cell is intended to act as a quick check on the health of the electroplating bath. Using the cell in conjunction with chemical analysis, it is possible to qualitatively and quantitatively analyze all of the major constituents of the bath. Consider the Hull cell as shown in Fig. 4. Major effort has been contributed towards the computation of current distribution in the Hull cell [25]. The dimensionless governing equation for the dimensionless potential inside the hull cell is given by $\nabla^2 \phi = 0$.

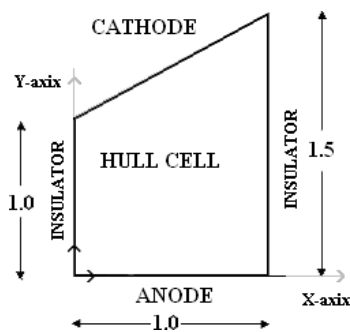


Figure 4. Schematic diagram of a Hull cell.

For this geometry, the Laplace equation is subjected to the following conditions:

$$\frac{\partial \phi}{\partial x} = 0 \quad \text{at insulators} \quad (11\text{-a})$$

$$\Phi = 10 \quad \text{at cathode} \quad (11\text{-b})$$

$$\Phi = 0 \quad \text{at anode (primary)} \quad (11\text{-c})$$

$$-\frac{\partial \phi}{\partial y} = J_a \phi \quad \text{at anode (secondary linear)} \quad (11\text{-d})$$

$$-\frac{\partial \phi}{\partial y} = J_a [\exp(-0.5\phi) - \exp(0.5\phi)] \quad \text{at anode (secondary nonlinear)} \quad (11\text{-e})$$

where J_a is the polarization parameter.

3.5 Curvilinear Hull Cell

Consider current flow between planar electrodes placed on two radii of an annular section, forming a cell with concentric cylindrical walls as shown in Fig. 5 [26]. The curved walls are insulators and there are no variations in the axial direction of the cylindrical coordinate system. The anode is reversible and the expression for the cathodic reaction kinetics is linear. The governing equation, in dimensionless form, is:

$$\frac{1}{\rho} \frac{\partial}{\partial \rho} \left[\rho \frac{\partial \phi}{\partial \rho} \right] + \frac{1}{\rho^2} \frac{\partial^2 \phi}{\partial \theta^2} = 0 \quad (12)$$

with the boundary conditions:

$$\frac{\partial \phi}{\partial \rho} = 0 \quad \text{at } \rho = 1 \quad (12\text{-a})$$

$$\text{and } \frac{\partial \phi}{\partial \rho} = 0 \quad \text{at } \rho = 3 \quad (\text{insulator}) \quad (12\text{-b})$$

$$\phi = 0 \quad \text{at } \theta = \frac{\pi}{2} \quad (\text{anode}) \quad (12\text{-c})$$

and

$$\phi - \frac{P}{\rho} \frac{\partial \phi}{\partial \rho} = 1 \quad \text{at } \theta = 0 \quad (\text{cathode with linear kinetics}) \quad (12\text{-d})$$

where P is the polarization parameter.

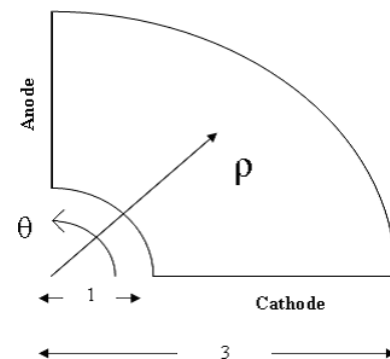


Figure 5. Schematic diagram of a curvilinear Hull cell.

3.6 Thin Layer Galvanic Cell

Consider the thin layer galvanic cell as shown in Fig. 6 [27]. The Laplace equation can be written in dimensionless form as:

$$\frac{\partial \phi}{\partial y^2} + \epsilon^2 \frac{\partial^2 \phi}{\partial x^2} = 0 \quad (13)$$

where $\epsilon = W/L$ is the aspect ratio with the insulator boundary conditions at $x = 0$ and 1 , and $y = 1$. The boundary condition at $y = 0$ is given by:

$$\frac{\partial \phi}{\partial y} = J_a \epsilon^2 \phi \quad 0 \leq x \leq a \text{ at the anode} \quad (13\text{-a})$$

and

$$\frac{\partial \phi}{\partial y} = J_c \epsilon^2 (\phi - 1) \quad a \leq x \leq 1 \text{ at the cathode} \quad (13\text{-b})$$

where a is the ratio of the anode length to the total length of the cathode.

3.7 Recessed Disc Electrode

The primary current distribution and ohmic resistance are evaluated for a disc electrode recessed in an insulating plane (see Fig. 7). The analysis can also be used to determine the ohmic resistance to flow of current through a pore of a separator. The primary current distribution is valid when concentration variations are negligible and when the resistance of the interfacial reaction is zero. For these conditions, the distribution of current density and potential is given by Laplace's equation. The boundary conditions are:

$$\phi = 0, \text{ as } z^2 + r^2 \quad (14\text{-a})$$

$$\phi = V, \text{ at } z = 0 \text{ and } r < r_0 \quad (14\text{-b})$$

$$\frac{\partial \phi}{\partial z} = 0, \text{ at } z = L \text{ and } r > r_0 \quad (14\text{-c})$$

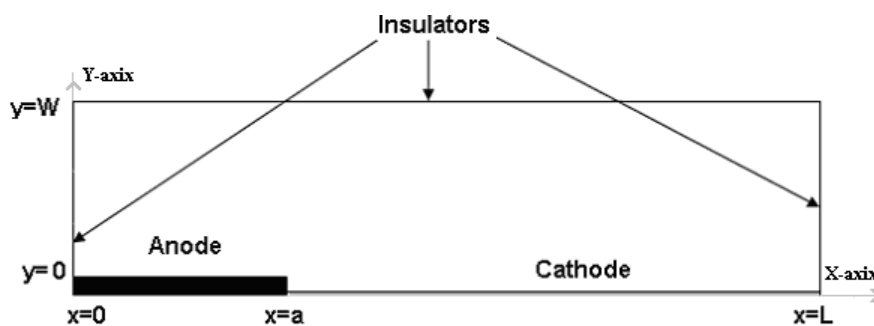


Figure 6. Schematic diagram of a thin layer galvanic cell.

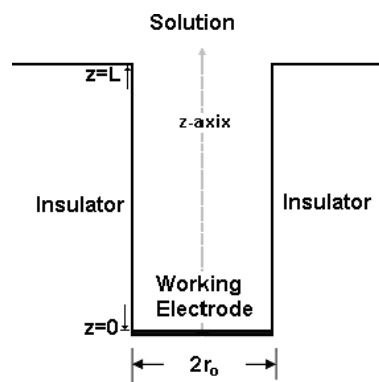


Figure 7. Schematic diagram of a recessed disc electrode.

and

$$\frac{\partial \phi}{\partial r} = 0, \text{ at } r = r_0 \text{ and } 0 < z < L \quad (14\text{-d})$$

The outer radius of the insulating plane (at $z = L$) is assumed to be much larger than r_0 . The above geometry's two-dimensional analogue, given by Diem et al. [28] (Fig. 8), is considered to be solved.

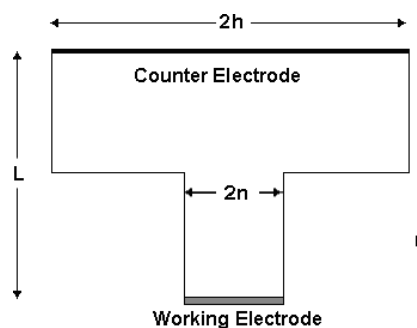


Figure 8. Two-dimensional analogue to Fig. 7.

4 Semi-Analytical Method

Many of the electrochemical systems require common calculation procedures to analyze tertiary current distribution irrespective of the cell geometry. The working electrode may take a different position with respect to the counter electrode, such as in the rectangular geometry where the electrodes are parallel or through-hole plating, where the electrodes are perpendicular. However, the potential drop due to activation polarization is constant in any geometry and, also, it is independent of position along the electrode. The basic computation methodology developed here is based on this constant and uniform activation polarization property

of the electrode, and power series solution assumption for convective diffusion. The main principle of the calculation procedure consists of assuming the series solution for the surface concentration and finding the expressions for evaluating the series coefficients. A scaling of all parameters that appear in the problem suggests that the results can be best presented in terms of the dimensionless quantities.

$$X = \frac{x}{L}; b^* = \frac{b}{L}; C_s^* = \frac{C_s}{C_\infty}; i^* = \frac{nF}{RT} \frac{L}{k} i \quad (15)$$

$$Q^* = \frac{nF}{RT} Q, \text{ where } Q = \eta_a, \eta_c, \phi_{\text{ohm}}, E$$

The calculation procedure for the more general case is presented below. It can be readily extended to any geometry of interest including the cases discussed in the previous section. Introducing the dimensionless quantities into the governing model equations, we have:

Voltage balance:

$$E^* = \Phi_{\text{ohm}}^* + \eta_a^* + \eta_c^* \quad (16)$$

Modified Butler-Volmer electrode kinetics:

$$i^* = J C_s^* \gamma [\exp(a \eta_a^*) - \exp(-\beta \eta_a^*)] \quad (17)$$

The transfer coefficients, a and β , are usually 0.5. The parameter, γ , is the electrochemical reaction order and it is 0.5. J is the dimensionless exchange current density and represents the ratio of the ohmic potential drop to the activation overpotential. A large value of J implies that the ohmic resistance tends to be the controlling factor for the current distribution.

Concentration overpotential:

$$\eta_c^* = \ln C_s^* \quad (18)$$

The analytical solution of the steady-state laminar convective diffusion can be obtained in three steps: (i) Apply the Laplace transformation to Eq. (4) assuming that the velocity component for the electrolyte along the y -direction is negligible, (ii) solve the resulting linear second-order ordinary differential equation with the corresponding boundary conditions of the given geometry, and (iii) use the convolution theorem and take the inverse Laplace transformation to get the complete solution. The resulting expression that relates the variables, surface concentration and the local current density, can be expressed as:

$$i^*(X) = N \int_0^X \left(\frac{dC_s^*}{dX} \right)_{X=t} \frac{dt}{(X-t)^q} \quad (19)$$

where t is a dummy variable, q is a constant ($0 < q < 1$), and N is a significant parameter called the average dimensionless limiting current density; both q and N depend upon the cell geometry and the corresponding boundary conditions used. The dimensionless form of the Laplace equation can be written as:

$$\nabla^2 \Phi^* = 0 \quad (20)$$

To solve the system of equations from Eq. (16) to Eq. (20), we have stated with the assumption of a power series for the surface concentration, the following:

$$C_s^* = \sum_{n=0}^{\infty} a_n X^{nq} \quad (21)$$

Here again q is a parameter which depends on the analytical solution of the convective diffusion equation, Eq. (19) (for the moving sheet process, $q = 1/2$, whereas it is $1/3$ for the other two examples considered). It can be noted that using the condition, $C_s(0) = C_\infty$, i.e., the bulk concentration of the reacting species, the series coefficient, a_0 equals 1.0. Taking the first derivative of Eq. (21) with respect to X , the current density distribution can also be expressed in terms of the assumed power series using Eq. (19):

$$i^*(X) = N \sum_{n=1}^{\infty} n a_n q X^{(n-1)q} \beta (1 - q, nq) \quad (22)$$

The modified Butler-Volmer electrode kinetics can be equated to the above series equation. The resulting expression is then used to calculate the numerical value of the other series coefficients. The expression is:

$$J C_s^* \gamma [\exp(a \eta_a^*) - \exp(-\beta \eta_a^*)] = N \sum_{n=1}^{\infty} n a_n q X^{(n-1)q} \beta (1 - q, nq) \quad (23)$$

$$\text{or } J \left[\sum_{n=0}^{\infty} a_n X^{nq} \right]^\gamma [\exp(a \eta_a^*) - \exp(-\beta \eta_a^*)] = N \sum_{n=0}^{\infty} (n+1) a_{n+1} q X^{nq} \beta (1 - q, (n+1)q) \quad (24)$$

Fig. 9 illustrates the technique in more detail. Despite the nested iterations, the convergence is very rapid. The procedure for evaluating series coefficients and, thus, the concentration and current distributions is detailed below for the case of a continuous moving sheet electrode process. The series solution assumption for the surface concentration on the continuous moving sheet electrode process is written as:

$$C_s^* = \sum_{n=0}^{\infty} a_n X^{\frac{n}{2}} \quad (25)$$

For this case, Eq. (19) reads (here $q = 1/2$ and $a_0 = 1.0$ based on the analytical expression for the convective diffusion equation):

$$i^* = N \int_0^X \left(\frac{dC_s^*}{dX} \right)_{X=t} \frac{dt}{\sqrt{X-t}} \quad (26)$$

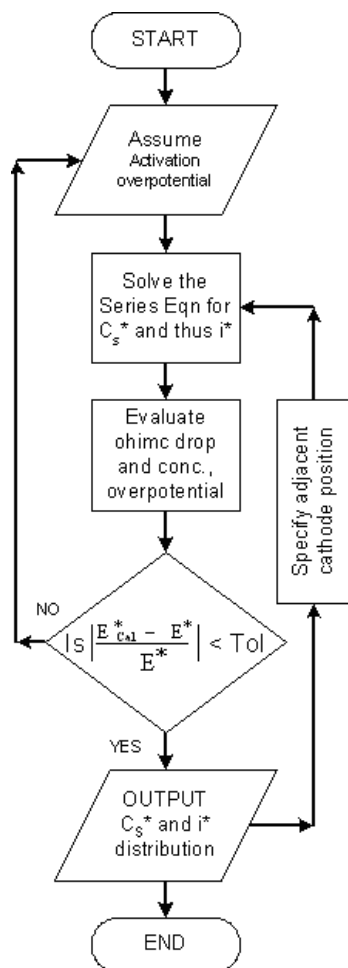


Figure 9. Outline of the algorithm used to solve the model equations using the semi-analytical method.

Using the series expression for surface concentration, we have from the above equation that the local current density can be expressed in series form as:

$$i^* = N \sum_{n=1}^{\infty} \frac{n}{2} a_n X^{\frac{n-1}{2}} \beta \left(\frac{n}{2}, \frac{1}{2} \right)$$

Eq. (17) reads:

$$i^* = J C_s^* \gamma [\exp(a \eta_a^*) - \exp(-\beta \eta_a^*)]$$

Equating the above two equations and then again equating the like terms of X , we can get the expressions to evaluate the series coefficients.

$$J \left[\sum_{n=0}^{\infty} a_n X^{\frac{n}{2}} \right]^{\gamma} [\exp(a \eta_a^*) - \exp(-\beta \eta_a^*)] \\ = N \sum_{n=1}^{\infty} \frac{n}{2} a_n X^{\frac{(n-1)}{2}} \beta \left(\frac{1}{2}, \frac{n}{2} \right)$$

$$a_1 N \frac{1}{2} \beta \left(\frac{1}{2}, \frac{1}{2} \right) = J Y a_0^{\gamma}$$

$$a_2 N \frac{1}{2} \beta \left(1, \frac{1}{2} \right) = \gamma J Y a_0^{\gamma-1} \frac{a_1}{2}$$

$$a_3 \frac{3N}{2} \beta \left(\frac{3}{2}, \frac{1}{2} \right) = \gamma(\gamma-1) J Y a_0^{\gamma-2} \frac{a_1}{2} + \gamma J Y a_0^{\gamma-1} \frac{a_1}{2}$$

$$a_4 \frac{3N}{2} \beta \left(2, \frac{1}{2} \right) = \gamma(\gamma-1)(\gamma-2) J Y a_0^{\gamma-3} \frac{a_1^3}{8} + 2\gamma(\gamma-1) J Y a_0^{\gamma-2} \\ \times \frac{a_2}{2} + \gamma(\gamma-1) J Y a_0^{\gamma-1} \frac{a_1}{2} \frac{a_2}{2} + \gamma J Y a_0^{\gamma-1} \frac{3a_3}{4}$$

where $Y = -\{\exp(a \eta_a^*) - \exp(-\beta \eta_a^*)\}$.

Assuming a value for activation polarization, the surface concentration can be calculated at any given position on the electrode using the above four equations and $a_0 = 1.0$. This is a series evaluation. The corresponding local current density distribution is calculated from the electrode kinetics expression. The concentration overpotential can be calculated from Eq. (18). Next, using the evaluated current density, the ohmic potential drop can be computed from the analytical solution of the Laplace equation for the respective geometry. Next, with all the overpotentials in hand, the cell potential, E^* , is calculated based on the output from the initially guessed activation overpotential. If the absolute value of the relative percent difference between the calculated and specified cell potential is greater than the specified tolerance (10^{-4}), then the activation polarization is adjusted and the procedure repeated until convergence. If the absolute value of the relative percent difference is less than the specified tolerance, the activation polarization is recorded and the governing equations for average current density and limiting current density are calculated, and quite a few cases have already been demonstrated by this procedure [9]. The major differences and advantages of this procedure are: the developed method involves iteration for only one variable instead of the doubly iterative calculation procedure used in the conventional methods; the assumption of a power series solution for C_s^* is alone required in the present method, unlike an initial guess of the current distribution itself. Above all, the technique developed will open up the possibilities to model systems with irregular geometry, unusual boundary conditions or multi-ion electrodeposition. The second striking feature enables a very simple programming need for this methodology. This capability becomes very important because, if the tertiary current distribution is the main issue, the assumption of current density distribution can produce coding intricacy and conspicuous errors.

5 Implementation in FEMLAB

FEMLAB is a powerful tool with an interactive environment for modeling. It is the first engineering tool that performs

equation-based multiphysics modeling in an interactive environment. The FEMLAB, a commercial package, is a toolbox written in MATLAB and is used to solve the set of governing equations. It solves systems of coupled partial differential equations (PDE) of up to 32 independent variables. The specified PDEs may be nonlinear and time-dependent, and act on one-, two- or three-dimensional geometry. The geometry of the storage is defined. The equations are written in partial differential form in line with program definitions, and initial and boundary conditions are determined. The mesh convergence is verified with refined mesh sizes. A time step of 1000 s, 1866 nodes, and 8080 element mesh size were considered to be appropriate.

The FEMLAB provides a number of predefined partial differential equations (PDEs) from several areas of science and engineering (referred to as application modes). Additional models with specific PDEs can be defined. All equations are solved simultaneously by applying the finite element method (FEM). A specific documentation of all the abilities of FEMLAB can be found in the manuals [29]. These manuals provide the numerical solution strategy used in this work along with detailed information on the type of solvers and time-stepping procedure. Given the geometry data, an initial finite element mesh is automatically generated by triangulation of the domain. The mesh is used for discretization of the PDE problem and can be modified to improve accuracy. The geometry, PDEs, and boundary conditions are defined by a set of fields similar to the structure in the language C. A graphical user interface is used to simplify the input of these data. For solving purposes, FEMLAB contains specific solvers (like static, dynamic, linear, nonlinear solvers) for specific PDE problems.

The modeling calculation procedures for concentration and current distributions throughout the system using FEMLAB are:

- Choose the “PDE” in Model Navigator, select “2D”, and select “Convection and diffusion mode” for the convective diffusion equation and “Conductive media DC” for the Laplace equation in application mode from the Multiphysics menu.
- Draw the geometry.
- Set the boundary conditions.
- Add constants and expressions.
- Initialize the mesh.
- Solve the problem.
- If necessary, resize the mesh and solve again.

The computer used for the simulation in this work is a PC with a 1.8 GHz processor with a 1 GB RAM. The time cost varies from 30 min to 90 min depending on the case considered in the previous section.

The equations and boundary conditions were outlined in section 3. Furthermore, all equations for the calculation of interim values are supplied as expressions. Parameters and other constant values are entered as constants. FEMLAB uses a triangular mesh for 2D geometries. The results are calculated using the stationary nonlinear solver. The result is the current and concentration distribution of the system.

Furthermore, for all the simulation results presented in this paper, the default mesh generation and solver are used. The

simulation times are fast (order ~ seconds) for linear problems such as the 2D Hull cell, curvilinear Hull cell, etc. The problems are summarized in Tab. 1a) whereas the geometrical parameters considered and the physical constants used are given in the Tabs. 1b) and 2. The data of semi-analytical methods were used to validate the results obtained from FEMLAB methodology.

Table 1a). FEMLAB methodology.

Boundary	Conductive media DC mode	Convective diffusion mode
1. Continuous moving electrode		
Anode	$V = 0$	$Ci = 1$
Cathode	Inward current density, $g = c$	$-Nin = -C$
Wall ($x = 0$)	Insulation/symmetry	$Ci = 1$
Wall ($x = L$)	Insulation/symmetry	Convection/diffusion
2. Through-hole plating		
Anode	$V = 0$	$Ci = 1$
Cathode	Inward current density, $g = C$	$-Nin = -C$
Walls	Insulation/symmetry	$Ci = 1$
3. Plane parallel electrode		
Anode	$V = 0$	$Ci = 1$
Cathode	Inward current density, $g = C$	$-Nin = -C$
Wall ($x = 0$)	Insulation/symmetry	$Ci = 1$
Wall ($x = L$)	Insulation/symmetry	Convection/diffusion
4. Hull cell		
Anode	$V = 0$ (primary), $g = -J_a * V$ (secondary linear)	
Cathode	$V = 10$	
Walls	Insulation/symmetry	
5. Curvilinear Hull cell		
Anode	$V = 0$	
Cathode	$g = -x/0.001$ and $q = -x/0.001$	
Walls	Insulation/symmetry	
6. Thin layer galvanic cell		
Anode	$g = -10 V$	
Cathode	$g = -10 (V-1)$	
Walls	Insulation/symmetry	
7. Recessed disc electrode		
Anode	$V = 0$	
Cathode	$V = V$	
Walls	Insulation/symmetry	

Table 1b). Geometrical parameters used in the model simulation.

Moving Electrode Process			
Length of the cell	L	400 cm	[8]
Height of the cell	b	300 cm	»
Velocity of the moving electrode	U_s	2.5 cm s^{-1}	»
Through-hole Plating Process			
Through-hole length	L	0.8 cm	[9]
Through-hole radius	R_0	0.04–0.20 cm	»
Plane Parallel Electrode Process			
Height-to-electrode length ratio	b/L	0.5–1.0	[14]
Hull cell			
Potential at Cathode	Φ	10	[15]
Curvilinear Hull Cell			
Polarization parameter	P	1	[15]
Thin Layer Galvanic Cell			
Aspect ratio	ϵ	0.001	[15]
Recessed disc electrode			
Dimensions	$h/(L-m)$	1.622	[18]
	h/n	5.0	[18]

Table 2. Physicochemical and kinetic parameters employed in the model simulation.

Parameter	Symbol	Value	References
Conductivity of bulk solution	κ	$0.4 \text{ } \Omega \text{ cm}^{-1}$	[2]
Diffusivity [copper]	D	$5.2 \cdot 10^{-6} \text{ cm}^2 \text{ s}^{-1}$	»
Cathodic transfer coefficient	β	0.5	»
Anodic transfer coefficient	α	0.5	»
Electrochemical reaction order	γ	0.5	»
Cell temperature	T	303 K	»
Electrolyte feed flow rate	U	25 cm s^{-1}	»
Exchange current density	i_0	1.0 A cm^{-2}	»
Bulk concentration of reactant	C_∞	1.0 mol cm^{-3}	»
Average velocity of electrolyte	$\langle V \rangle$	25.0 cm s^{-1}	»
Electrons produced/reactant ion	n	2	»
Cell geometry dependent constant	q	$0 < q < 1$	–
Universal gas constant	R	$8.314 \text{ J mol}^{-1} \text{ K}^{-1}$	–
Faraday constant	F	$96\,487 \text{ C mol}^{-1}$	–

6 Results and Discussion

6.1 Continuous Moving Sheet Electrode

Fig. 10a) shows the current distribution for a continuous moving sheet electrode. The current density is highest at the leading edge where the concentration boundary layer is thin and the rate of mass transfer is high; then the concentration boundary layer grows gradually from the leading edge and the current density decreases. At the trailing edge, the effect of the concentration boundary layer is important and the current density becomes lesser.

Fig. 10b) presents the surface concentration distribution. The concentration effects increase with current density due to mass transfer limitations. The surface concentration is equal to

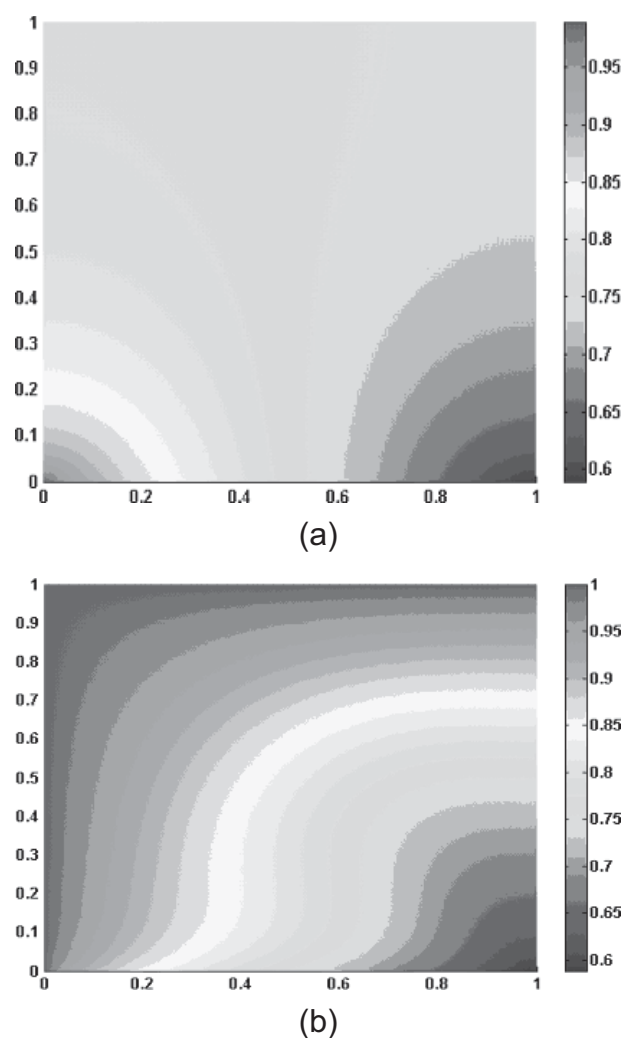


Figure 10. (a) Current density distribution for the continuous moving sheet electrode process. (b) Dimensionless surface concentration distribution for the continuous moving sheet electrode process.

the bulk concentration at the leading edge and decreases sharply with increasing distance along the electrode. The surface concentration distribution can be uniform for the smallest current. Current distribution strongly depends on the magnitude of the limiting current. The results are presented for the first-order kinetics. A uniform current density can be achieved if the average current density at the electrode is less than 78.5% of the average limiting current density.

6.2 Electroplating of a Through-Hole

Typical electrolyte, kinetic, mass-transfer, and geometric parameters encountered during copper deposition onto multi-layered printed circuit boards are given in Tab. 2. We assume symmetry of the anode position and agitation on both sides of the board, and then the results are plotted for the entire surface of the through-hole. Fig. 11a) is the graphical representation of calculated dimensionless surface concentration

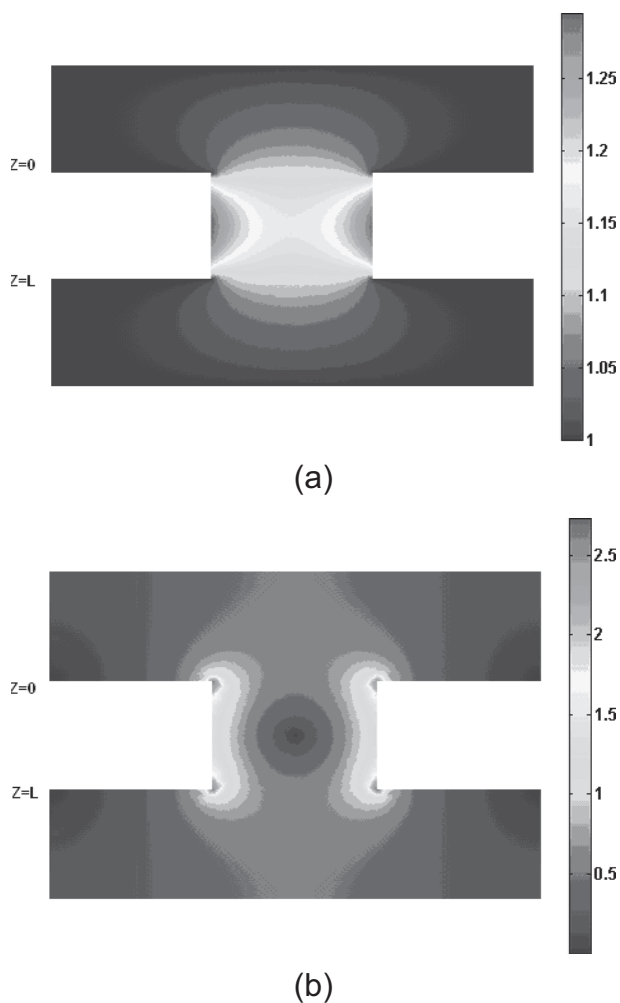


Figure 11. (a) Calculated surface concentration distributions within a through-hole. (b) Current density distribution within a through-hole.

distribution. At relatively low values of applied potential, the current distribution depends on the cell geometry, the charge transfer characteristics of the electrochemical reaction, and the electrolyte conductivity. In this situation, the current density is highest at both ends of the through-hole because they are nearer to the counter electrodes. As the applied potential is increased, the solution inside the through-hole becomes depleted in the reacting species. Consequently, the edges of the through-hole are more accessible to the counter electrode and are constantly being supplied with the reacting species. Accordingly, they become more reactive with respect to the interior regions as the applied potential is increased. This causes the current distribution to become increasingly non-uniform, as shown in Fig. 11b). The potential difference decreases from the value at each end toward the middle of the through-hole. As a result, the concentration and potential profiles counteract each other for the downstream half of the through-hole.

6.3 Plane Parallel Electrodes

The simulation data describing the cathode process is given in Tab. 2. Fig. 12a) shows the current distribution. Near the front of each electrode, the current drops rapidly, behaving like a secondary current distribution. However on the cathode, mass transfer effects become more important with increasing x . The limiting current occurs when the current distribution is limited by the mass transfer rate through the diffusion layer and secondary current distributions occur when there is a surface overpotential but no mass transfer effects. The concentration distribution for the system is shown in Fig. 12b). The cathodic current cannot continue to behave like a secondary current because the reactant concentration has been reduced inside the diffusion layer. For the cathode, the concentration drops rapidly at the front of the electrode. This behavior is caused by the rapid depletion of reactant at the beginning. However, after the current has dropped, the concentration has chance to increase by diffusion into the diffusion layer; but concentration effects are relatively unimportant on the anode and the anodic current continues to resemble a secondary current distribution.

6.4 Hull Cell

The primary current distribution throughout the system (for unit conductivity, k) is shown in Fig. 13a) and for the anode, it is shown in Fig. 13b).

The linear kinetics secondary current distribution at the anode is obtained and shown in Fig. 13c) (for unit conductivity). For various values of polarization parameter, J_a , the distribution is plotted. Note that as J_a increases, primary current distribution is approached (Fig. 13d)).

The secondary nonlinear current distribution in the system is shown in Fig. 13e) and the distribution in the anode is plotted in Fig. 13f). For higher values of the polarization parameter, J_a , the primary current distribution is obtained as expected.

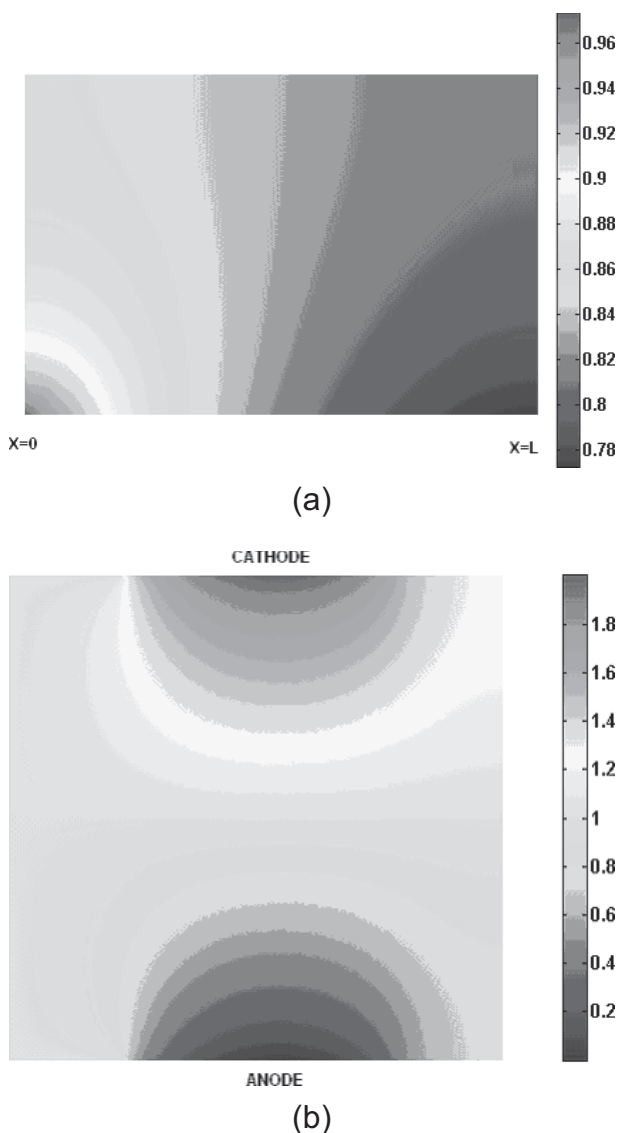


Figure 12. (a) Dimensionless current distribution for a plane parallel electrode process. (b) Surface concentration distribution for a plane parallel electrode process.

6.5 Curvilinear Hull Cell

The current distribution is shown in Fig. 14. All the plots given in [16] for different polarization parameters can be completely reproduced with our solution technique by merely solving with P as a parameter in the boundary condition. The current distribution is found as a function of geometric ratios and a dimensionless polarization parameter. It is suggested that a cell of this geometry may be used to measure quantitative throwing power as well as to observe qualitative properties of plating-bath solutions.

6.6 Thin Layer Galvanic Cell

The potential distribution is obtained by solving Eq. (12), which is shown in Fig. 15a) for $a = 0.2$ and $\epsilon = 0.001$. Secondary current distributions for different values of the polarization parameters are plotted in Fig. 15b). Also, a similar boundary value problem arising in a cylindrical thin layer galvanic cell [27] can be solved easily using our technique.

6.7 Recessed Disc Electrode

The ratio m/n is analogous to L/r_0 . Since, in two dimensions, currents cannot flow to infinity without an infinite potential drop, the counter electrode is placed at a finite distance from the working electrode. Placing the counter electrode too close to the working electrode distorts the current distribution on the supposedly “isolated working electrode”. The primary current distribution is shown in Fig. 16. The results can be used to design a cell that would have an approximately uniform current distribution in the absence of concentration variations. With convection, the mass transfer limited current distribution can be non-uniform.

7 Conclusion

The mathematical software FEMLAB approach that calculates the simplified current density distribution and concentration profiles of an electrochemical cell is presented. The results are validated by referring to the previously reported experimental and theoretical results as well as using the semi-analytical software approach that is presented in section 4. The models used are based on the successful theories and principles of electrochemistry that can capture all the activities involving electrochemistry in the industrial processes. The method requires no coding to solve for steady-state convective diffusion. Moreover, within the context of its limitations, this computational method can be extended to treat various cell operational modes. Seven test problems from classical electrochemical engineering are solved and discussed. Surface concentration and current density distribution on the electrode are computed for a continuous moving electrode, plane parallel electrode, and through-hole plating processes. The latter systems are solved for primary and secondary current distributions.

Acknowledgements

We acknowledge the Director, Central Electrochemical Research Institute, Karaikudi (India) for his constant encouragement.

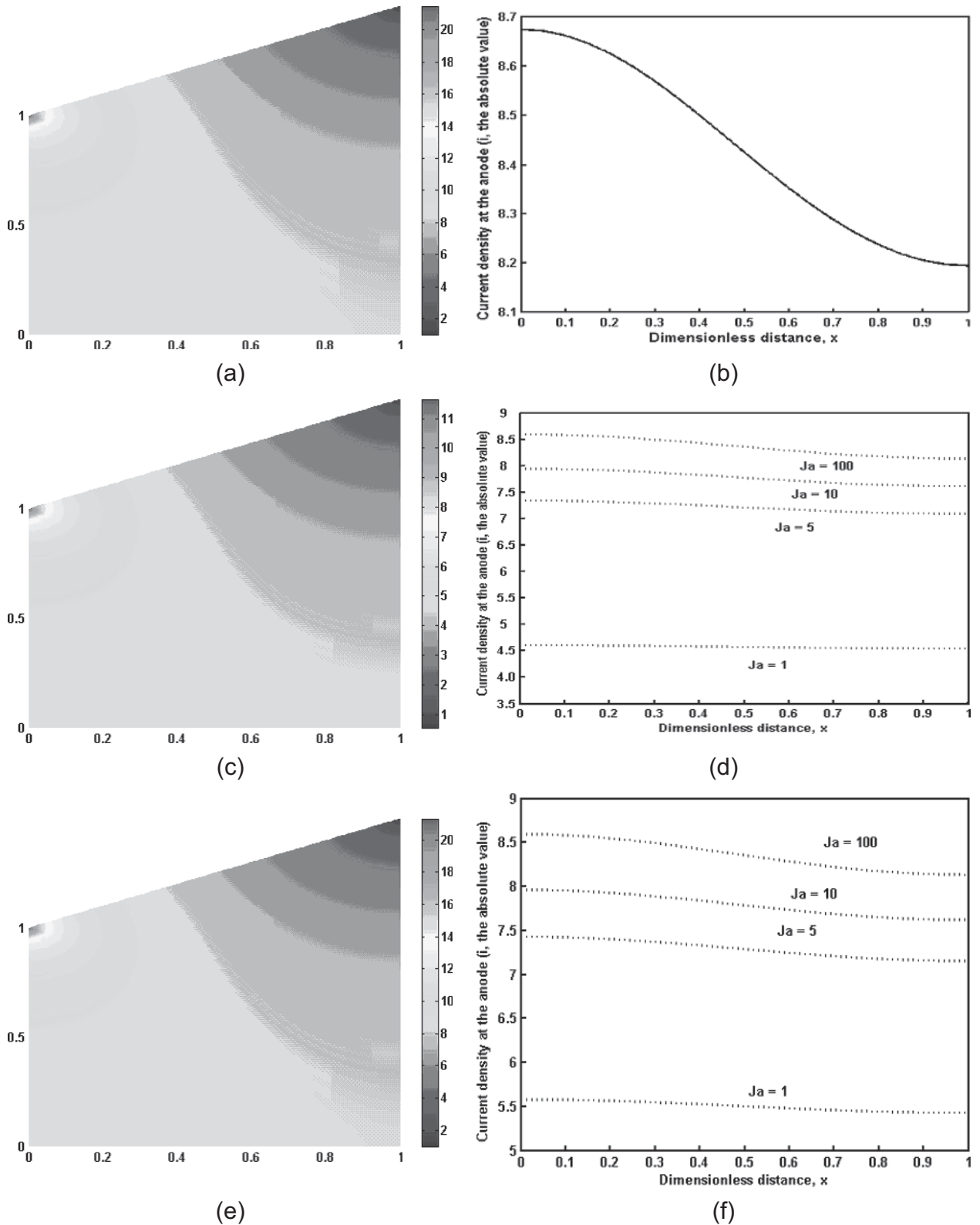


Figure 13. (a) Primary current density distribution in a Hull cell. (b) Primary current density distribution at the anode. (c) Linear Kinetics – Secondary current density distribution in a Hull cell (polarization parameter, $J_a = 1$). (d) Linear Kinetics – Secondary current density distribution in a Hull cell, effect of polarization parameter, J_a . (e) Nonlinear secondary current density distribution in a Hull cell (polarization parameter, $J_a = 100$). (f) Nonlinear secondary current density distribution in a Hull cell for Butler-Volmer boundary conditions.

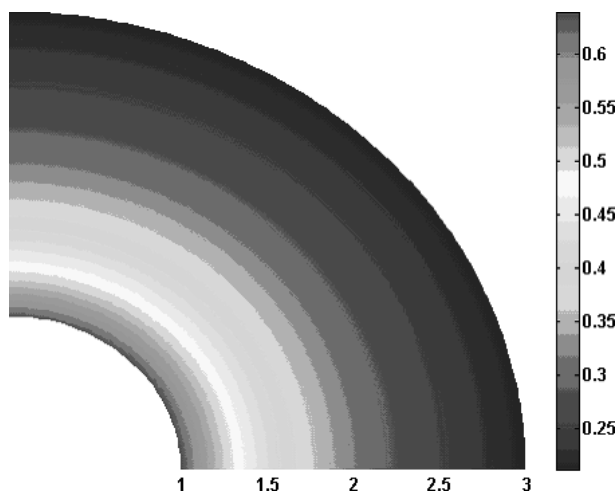
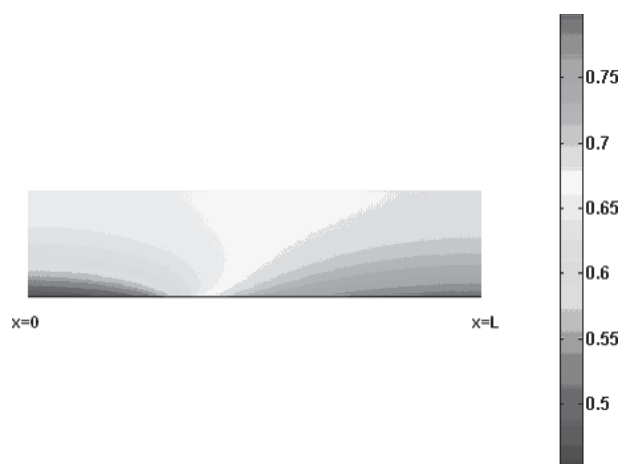


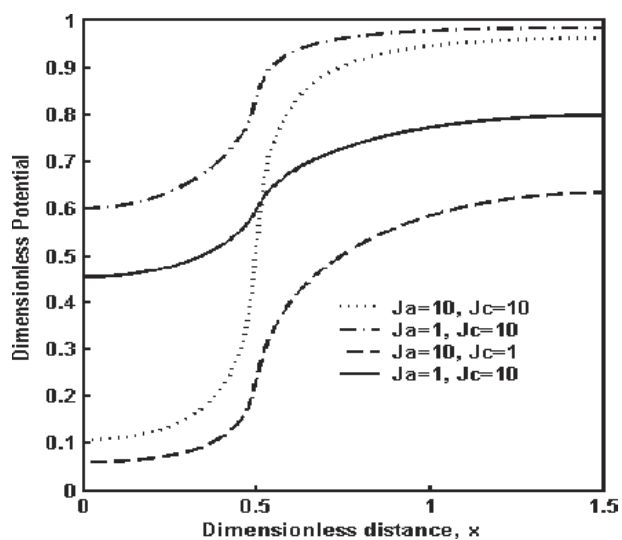
Figure 14. Secondary current density distribution on a curvilinear Hull cell ($P = 1$).

Symbols used

b	[m]	distance between the counter electrode and the working electrode
b^*	[-]	dimensionless electrode distance defined as b/L
C	[g-mole L ⁻¹]	concentration of the reacting ion
C_∞	[g-mole L ⁻¹]	bulk concentration of the reacting ion
C_s	[g-mole L ⁻¹]	concentration of the reacting ion
C_s^*	[-]	dimensionless concentration of the reacting ion
D	[m ² s ⁻¹]	diffusion coefficient of the reacting ion
E	[V]	difference between the applied cell voltage and the thermodynamic equilibrium cell voltage
E^*	[-]	dimensionless applied cell voltage
F	[C/equiv]	Faraday constant, $F = 96,487$ C/equiv
i	[A cm ⁻²]	local current density at the electrode
i^*	[A cm ⁻²]	dimensionless local current density at the electrode
i_o	[A/cm ⁻²]	exchange current density based on the bulk concentration
i_{avg}^*	[-]	dimensionless average local current density
i_{lim}	[A cm ⁻²]	local limiting current density
i_{lim}^*	[-]	dimensionless local limiting current density
J	[-]	dimensionless exchange current density
L	[m]	length of the electrode in the cell



(a)



(b)

Figure 15. (a) Linear secondary current density distribution in a thin layer galvanic cell ($J_a = 1, J_c = 1$). (b) Linear secondary current density distribution in a thin layer galvanic cell, effect of polarization parameter, J_c .

l	[-]	dimensionless through-hole radius, R_0/L
n	[-]	number of electrons transferred in the electrochemical reaction
N	[-]	average dimensionless limiting current density
q	[-]	a constant dependent on the cell geometry
Q	[-]	dummy variable used to symbolize the types of potentials
R	[J/(mol K)]	universal gas constant, $R = 8.3143$ J/(mol K)
R_0	[cm]	radial coordinate extending from the through-hole

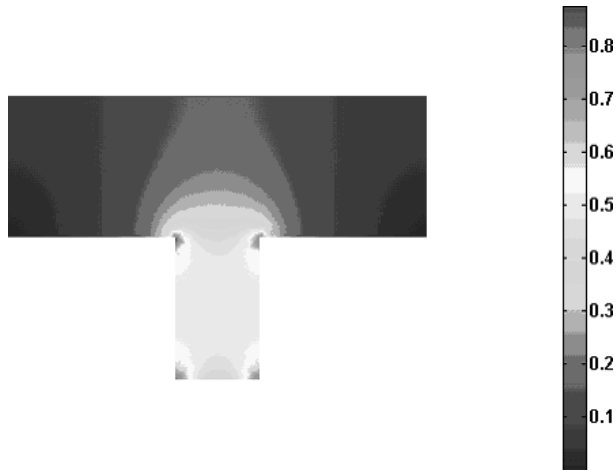


Figure 16. Primary current distribution in a recessed disc electrode.

T	[K]	temperature
U	[m s ⁻¹]	velocity component of the electrolyte along the x -direction
U_s	[m s ⁻¹]	velocity of the continuous moving sheet electrodes
$\langle U \rangle$	[m s ⁻¹]	average velocity of the electrolyte along the surface coordinate
$\langle V_z \rangle$	[m s ⁻¹]	average electrolyte velocity in the axial direction
V	[m s ⁻¹]	velocity component of the electrolyte along the y -direction
V_z	[m s ⁻¹]	axial component of the electrolyte velocity
X	[-]	dimensionless surface coordinate, x/L
Y	[-]	dimensionless axial coordinate extending from the through-hole wall surface, $(R_0 - R/R_0)$

Greek letters

Φ	[V]	electrode potential in the electrolyte phase
γ	[-]	an electrochemical parameter related to the order of the reactions
α, β	[-]	transfer coefficients
η_a	[V]	activity overpotential
η_c	[V]	concentration overpotential
κ	[mho/cm]	conductivity of the electrolyte
Φ_{ohm}	[V]	ohmic loss in the electrolyte phase between the counter electrode and the plane working surface
η_a^*	[-]	dimensionless activity overpotential
η_c^*	[-]	dimensionless concentration overpotential
Φ_{ohm}^*	[-]	dimensionless ohmic loss in the electrolyte phase between the

Φ^* [-]

counter electrode and the plane working surface
dimensionless ohmic loss in the electrolyte phase between the counter electrode and the panel surface

References

- [1] J. Newman, *Ind. Eng. Chem.* **1968**, *60* (4), 12.
- [2] J. Newman, *Electrochemical Systems*, Prentice Hall – Englewood Cliffs, New Jersey **1991**.
- [3] M. H. Chung, *Electrochim. Acta.* **2000**, *45* (24), 3949.
- [4] V. R. Subramanian, R. E. White, *J. Electrochem. Soc.* **2000**, *147*, 1636.
- [5] V. Boovaragavan, V. R. Subramanian, *J. Power Sources* **2007**, *173* (2), 1006.
- [6] V. R. Subramanian, V. Boovaragavan, V. Diwakar, *Electrochem. Solid-State Lett.* **2007**, *10* (11), A255.
- [7] V. Boovaragavan, V. R. Subramanian, *Electrochem. Commun.* **2007**, *9* (7), 1772.
- [8] V. R. Subramanian et al., *Electrochem. Solid-State Lett.* **2007**, *10* (2), A25.
- [9] V. Boovaragavan, C. Ahmed Basha, *J. Appl. Electrochem.* **2006**, *36* (7), 745.
- [10] V. Boovaragavan, C. Ahmed Basha, *J. Power Sources* **2006**, *158* (1), 710.
- [11] B. Vijayasekaran, C. Ahmed Basha, *Chem. Eng. J.* **2006**, *117* (3), 213.
- [12] B. Vijayasekaran, C. Ahmed Basha, *Electrochim. Acta.* **2005**, *51* (2), 200.
- [13] B. Vijayasekaran, C. Ahmed Basha, *Trans. SAEST* **2005**, *40* (1), 1.
- [14] V. Boovaragavan, C. Ahmed Basha, N. Balasubramanian, *Chem. Biochem. Eng. Q.* **2004**, *18* (4), 337.
- [15] V. Boovaragavan, C. Ahmed Basha, *Bull. Electrochem.* **2004**, *20* (3), 133.
- [16] M. Georgiadou, *Electrochim. Acta* **2003**, *48* (27), 4089.
- [17] S. H. Chan, H. Y. Cheh, *Chem. Eng. Commun.* **2004**, *191* (7), 881.
- [18] I. Rousar, V. Mejta, V. Cezner, *Chem. Eng. Sci.* **1980**, *35* (3), 717.
- [19] C. F. Coombs, *Coombs' Printed Circuits Handbook*, 5th ed., McGraw-Hill Professional, New York **2001**.
- [20] C. Fu, I. C. Ume, D. L. McDowell, *Finite Elem. Anal. Des.* **1998**, *30* (1–2), 1.
- [21] R. B. Bird, W. E. Stewart, E. N. Lightfoot, *Transport Phenomena*, Wiley, New York **1960**.
- [22] J. M. Bisang, *J. Appl. Electrochem.* **1997**, *27* (4), 379.
- [23] G. Nelissen et al., *J. Electroanal. Chem.* **2004**, *563* (2), 213.
- [24] A. A. Wragg, A. A. Leontaritis, *Chem. Eng. J.* **1997**, *66* (1), 1.
- [25] J. Lee, T. W. Chapman, *J. Electrochem. Soc.* **1998**, *145* (9), 3042.
- [26] R. Morris, W. Smryl, *J. Electrochem. Soc.* **1989**, *136* (11), 3229.
- [27] C. B. Diem, B. Newman, M. E. Orazem, *J. Electrochem. Soc.* **1988**, *135* (10), 2524.
- [28] *FEMLAB Reference Manual*, Stockholm **2003**.
- [29] *FEMLAB Users Guide and Introduction*, Stockholm **2003**.